# Laminar flame speed correlations for dual fuel flames in high-pressure conditions

Luís Eduardo de Albuquerque Paixão e Freire de Carvalho<sup>a,\*</sup>, Fernando Luiz Sacomano Filho<sup>a</sup> *a Laboratory of Environmental and Thermal Engineering, Universidade de São Paulo, São Paulo, Brazil.* 

#### **Abstract**

The usage of methane as a fuel stands out as a transition strategy to zero carbon energy conversion processes. However, methane is difficult to be made to burn due to its strong molecular structure. To mitigate this issue, a mixture of methane and a more ignitable fuel may be a promising solution for large scale combustion applications. In many of those, the corresponding CFD setup can be very demanding and detailed chemistry may be replaced by simplified approaches, such as laminar flame speed methods. To contribute with robust and reliable modeling of combustion processes fueled by dual fuel mixtures, novel formulations are proposed to improve accuracy of laminar flame speed correlations. To accomplish this task, numerical simulations of 1D freely propagating laminar flames based on detailed chemistry are conducted for various pressures and equivalence ratios. Kinetic mechanisms are obtained from the literature and evaluated with available experimental data. For the best performing mechanism, the resulting laminar flame speeds are mapped based on fresh mixture composition and correlated through power-law wholly empirical equations. The proposed formulations show clear improvements when compared to other existing methods. *Keywords:* dual-fuel combustion, methane-slip, flame speed, empirical correlation, diesel surrogate.

#### 1. Introduction

Combustion processes are present in various economic sectors and on diverse scales, making the thermal matrix essential to meet the world's energy demand. However, combustion is also associated with the production of greenhouse gases (GHG), as well as with the emission of pollutants, so that environmental and health concerns arise. In this context, it is essential to develop new technologies that support the worldwide increasing energy demands [1], while focusing on the mitigation of GHG and pollutant emissions. Herein, the combustion of methane stands out.

The relevance of methane combustion is due to its high hydrogen-to-carbon ratio. This aspect attenuates carbon dioxide emissions when compared to other fossil fuels. However, its chemical composition also implies greater chemical stability. As a result, fuel ignition may not optimally occur and a portion of methane may remain unburnt, being rejected into a flue gas stream (methane slip). To mitigate this phenomenon, a more ignitable fuel can be mixed with methane so that the triggering of combustion reactions is facilitated.

In typical combustion applications, such as internal combustion engines, the computational setup can be very demanding and even unfeasible when accounting for detailed chemistry modeling [2–6]. Therefore chemistry simplification methods are often preferred in complex numerical simulations, such as laminar flame speed methods [2, 5, 7–10]. As pointed out in the literature [11, 12], the laminar flame speed is a very relevant and representative property related to premixed combustion as it is directly connected with energy release rate, quenching, flame stabilization, performance, emissions and other relevant phenomena essential to combustion applications. Laminar

<sup>\*</sup>Corresponding author

Email address: luis.eduardo.carvalho@usp.br (Luís Eduardo de Albuquerque Paixão e Freire de Carvalho)

flame speed calculation can also be instrumental in the context of tabulated chemistry [13]. As an input of such methods, laminar flame speed may be obtained from different sources. It is useful to tabulate experimental results or to correlate laminar flame speed data into a representative equation, as is usually preferred for practical engine simulations [6]. However, laminar flame speed experimental data can be scarce for very specific applications, such as dual fuel blends. Such unavailability is even more pronounced when engine relevant conditions are sought.

Laminar flame speed correlations may be semi or wholly empirical. Although better supported by the underlying physics, semi-empirical correlations have been known to be overly sensitive to thermodynamic models. Also, some parameters of these correlations may not consistently depend on the variables used for regression. As a result, it may be very difficult to obtain smooth laminar flame speed profiles through the use of semi-empirical correlations. Therefore, wholly empirical correlations have been frequently preferred throughout the years [6, 7]. Frequently, these correlations describe laminar flame speeds as a function of equivalence ratio, pressure, temperature and fuel mixture composition [6, 7, 12, 14–26].

Broad information regarding applications and shortcomings of empirical laminar flame speed correlations can be found in the literature [6, 7, 25, 26]. Among such shortcomings, the common use of low order polynomials to approximate complex non-polynomial distributions of parameters can be highlighted [6, 7]. Furthermore, the regression of laminar flame speed data at varied pressure, temperature, and exhaust gas concentration usually yields highly scattered distributions of regression parameters in respect to equivalence ratio. This may be justified by the dependency of such parameters on variables other than equivalence ratio [25]. Additional dependencies of the regression parameters on variables such as pressure, temperature, exhaust gas concentration,

and fuel composition have already been suggested, but those have not been extensively analyzed [6, 25]. Herein, focus is given to power-law based wholly empirical laminar flame speed correlations accounting for pressure and fuel composition variations. Specifically, the dependence of the pressure exponent on these variables is explored.

In view of the above aspects, the investigation of the flame propagation speed in mixtures of n-heptane (diesel surrogate), methane and air in varied compositions, with different kinetic mechanisms and under different pressure conditions is carried out in the present work. Special attention has been paid to the development of a dataset and to empirical correlations for the laminar flame speed in dual fuel blends. Firstly, to reach this objective, different reaction mechanisms are evaluated by means of comparisons with available experimental data for single fuel combustion. Secondly, the best performing mechanism is used to construct a dataset, which can be straightly used as an input for CFD simulations. Herein, the use of blending laws [27] for laminar flame speed predictions of methane/n-heptane blends is not explored. This is due to the scarcity of experimental data in the studied conditions and in order to avoid the introduction of additional uncertainty by associating blending laws with detailed chemistry calculations. Finally, empirical correlations are extended, proposed and analyzed for various scenarios. Although the investigations conducted here considered dual fuel mixtures of methane and a diesel surrogate, the applicability of the proposed formulations is general and it is not limited to these fuels and their mixtures.

The remaining of this manuscript is structured as follows. After this introduction, wholly empirical correlations are overviewed, establishing the theoretical foundation available in the literature and its limitations. Next, the methodology regarding laminar flame speed data calculations, their validation and correlation is presented. In the methodology section, the use of wholly

formulation of Hu et al. [23] is extended from a single equivalence ratio to the whole flammability range in both single and dual fuel conditions. The following results section is divided in two subsections, the first regarding detailed chemistry calculations, validation and mapping, and the second dedicated to the investigation of the chosen empirical correlations. In this second subsection, a new formulation for the pressure exponent is proposed in order to account for the influence of the fuel blend composition in dual fuel context.

## 2. Overview of wholly empirical correlations

80

Most wholly empirical correlations follow the form of a power-law

$$S_u = S_{u0}(T/T_0)^{\alpha} (P/P_0)^{\beta}. \tag{1}$$

From Eq. 1 and a laminar flame speed  $S_u$  dataset, the distributions of reference flame speed  $S_{u0}$ , temperature exponent  $\alpha$  and pressure exponent  $\beta$  can be obtained. These distributions are then subjected to subsequent correlations and may depend on pressure and temperature [6], as well as on other parameters such as fuel composition.

As proposed by Metghalchi and Keck [14],  $S_{u0}$  (Eq. 2),  $\alpha$  (Eq. 3) and  $\beta$  (Eq. 4) may be modeled as dependent only on the equivalence ratio  $\phi$  for a given reference condition ( $P_0$ ,  $T_0$ ),

$$S_{u0} = B_m + B_2(\phi - \phi_m)^2, \tag{2}$$

 $\alpha = \alpha_1 + \alpha_2(\phi - 1),\tag{3}$ 

$$\beta = \beta_1 + \beta_2(\phi - 1),\tag{4}$$

where  $B_m$ ,  $B_2$ ,  $\alpha_1$ ,  $\alpha_2$ ,  $\beta_1$ , and  $\beta_2$  are constants to be fitted to the corresponding datasets. In the original work of Metghalchi and Keck [14], the coefficients of Eqs. 3 and 4 do not depend on fuel composition. Characteristics of the fuel are embedded in the coefficients of Eq. 2. The coefficient  $\phi_m$  is obtained from another flame speed regression

$$S_u = C_m + C_2(\phi - \phi_m)^2, (5)$$

where  $C_m$  and  $C_2$  are also constants to be fitted to the corresponding dataset.

Given the shortcomings of the polynomial formulations used to correlate the reference flame speed, discussed by Amirante et al. [6], a different approach was proposed by Ömer L. Gülder [7]

$$S_{u0} = ZW\phi^{\eta}e^{-\zeta(\phi-\sigma)^2},\tag{6}$$

in which Z is unitary for single component fuels and W,  $\eta$ ,  $\zeta$ , and  $\sigma$  are fuel dependent constants.

Regarding fuel blends, Gulder's formulation was extended for binary and ternary mixtures (as presented by Dirrenberger et al. [20]), to account for the influence of additional components on the laminar flame speed peak's amplitude and position. However, as noted by Amirante et al. [6], additional components may impact the laminar flame speed in different extents depending on the equivalence ratio. Thus Amirante et al. [6] proposed a modified version of the equations presented by Dirrenberger et al. [20], which is the form that is used throughout this work (Eq. 7). In Eq. 7, the constants  $\nu$  and  $\tau$  characterize the dependence of Z on fuel composition. An additional exponential term  $\Omega$  is introduced to model the shift of the maximum flame speed resulting from the blend and  $\epsilon$  accounts for the equivalence ratio dependent sensitivity of laminar flame speed regarding an additional fuel component. The presence of the secondary fuel is quantified by its

molar fraction  $X_{2nd}$ :

105

$$S_{u0} = (1 + \nu X_{2nd}^{\tau}) W \phi^F \exp[-\zeta (\phi - \sigma - \Omega X_{2nd})^2], \text{ with } F = \eta (1 - X_{2nd})^{\epsilon}.$$
 (7)

Special attention is given hereafter to the temperature and pressure exponents,  $\alpha$  and  $\beta$ . Even though first proposed as linear functions of  $\phi$  by Metghalchi and Keck [14], second ( $\alpha_4 = \beta_4 = 0$ ) and third order polynomials are the most common forms to be found in the literature for these exponents

$$\alpha = \alpha_1 + \alpha_2 \phi + \alpha_3 \phi^2 + \alpha_4 \phi^3, \tag{8}$$

$$\beta = \beta_1 + \beta_2 \phi + \beta_3 \phi^2 + \beta_4 \phi^3. \tag{9}$$

Despite their supposed dependencies on pressure, temperature, fuel composition, and other parameters, not many studies have been found exploring them [18, 23–26]. In respect to the dependence of  $\beta$  on the pressure, the work of Hu et al. [23] is one of the few, if not the only one, to propose an empirical correlation (Eq. 11). This equation, however, is proposed for a single equivalence ratio, such that  $\beta$  is written only as a function of the pressure (in MPa). A linear equation for  $\alpha$  depending on the temperature was also proposed in the same paper

$$\alpha = \alpha_{T1} + \alpha_{T2}T,\tag{10}$$

$$\beta = \beta_{p1} e^{-P/\beta_{p2}} - \beta_{p3},\tag{11}$$

where  $\alpha_{T1}$ ,  $\alpha_{T2}$ ,  $\beta_{p1}$ ,  $\beta_{p2}$ , and  $\beta_{p3}$  are constants to be fitted. To the authors' knowledge the dependence of  $\alpha$  and  $\beta$  with the fuel composition for dual fuel mixtures remains a fairly unexplored subject, as no references discussing this topic were found.

## 3. Methodology

To investigate the behavior of empirical correlations for dual fuel combustion at different pressures, it is indispensable to consider a comprehensive dataset of laminar flame speed. However, the availability of this kind of information is scarce. To overcome this issue, detailed chemistry simulations of freely propagating flames are employed in this work.

In order to achieve reliable results, the detailed chemistry simulations are conducted in two stages: (1) the validation of the numerical setup coupled with the selected mechanisms and (2) the calculation of laminar flame speeds for dual fuel combustion, at different pressures, through the use of the best performing mechanism. Accordingly, the results are used to obtain empirical regressions that allow the concise representation of the constructed dataset of laminar flame speed for different methane/n-heptane blends at varied pressure conditions through two further steps: (1) single fuel power-law correlations and (2) dual fuel power-law correlations.

As well known, diesel is a multi-component fuel composed of many individual substances. Usually, such a complex fuel is simplified by a small number of substances, namely a surrogate [4]. In this work, diesel is represented by n-heptane, as done by Liu et al. [28].

For flame speed calculations, the kinetic mechanisms of Liu et al. [28], Chaos et al. [29] and of the Polytechnic University of Milan (Polimi) [30] are used. The skeletal n-heptane kinetic mechanism of Liu et al. [28] consists of 43 chemical species and 185 chemical reactions, counting each forward and backward reaction individually. It was developed to study diesel ignition phenomena and was validated through ignition delay time and Plug Flow Reactor (PFR) species profile data. The reduced mechanism of Chaos et al. [29] stems from a detailed version developed in the

same paper. As mentioned in [29], the reduced mechanism is composed of 107 species and 723 chemical reactions. It was developed for Primary Reference Fuels (PRF) and validated through laminar flame speed data, as well as PFR and Jet-Stirred Reactor (JSR) speciation profile data, for n-heptane, iso-octane, and PRF mixtures. Validation for shock tube ignition delay was also conducted, but only for n-heptane and iso-octane. Finally, Polimi's mechanism is composed of 254 species and 7568 reactions and was developed for Toluene Primary Reference Fuels (TPRF). It is important to mention that the CFD simulations presented here were conducted with the academic software Chem1D [31].

Table 1: Kinetic mechanisms' numbers of chemical species and reactions

Mechanism	Species	Reactions		
Liu et al. [28]	43	185		
Chaos et al. [29]	107	723		
Polimi [30]	254	7568		

In order to validate the numerical setup, experimental data for hydrocarbons presented by Davis and Law [32], Jerzembeck et al. [33], Kelley et al. [34], Hu et al. [23] and Li et al. [35] are used. One-dimensional freely propagating flames of methane and n-heptane blends, varying the fresh mixture composition, are simulated. As a first validation step, flames corresponding to the data of Davis and Law [32] are calculated with each mechanism under atmospheric pressure and  $T_0 = 298K$ . Simulations are performed between the numerical flammability limits, defined

here as  $S_u = 5$  cm/s, for different available diffusion transport models. After comparing the results obtained with the reference data of [32], the best performing mechanism is selected for laminar flame speed prediction, with a selected diffusion transport model, at high pressure in dual fuel combustion context.

An additional validation step for the selected numerical setup is performed through laminar flame speed experimental datasets of methane at elevated pressures [23], of n-heptane at elevated pressures [33, 34] and of methane/n-heptane blends at atmospheric pressure [35]. Although these validation cases do not exhaust relevant experimental datasets, good performance relative to such cases indicates the robustness of the numerical setup regarding equivalence ratio, blend composition and pressure variations.

155

170

To determine the coefficients of the empirical equations that replicate the flame velocity of single and dual combustion of methane and n-heptane at varying pressures, data was obtained for  $T_0 = 298$  K, mole fraction  $X_{CH_4} = \{0.0, 0.2, 0.4, 0.6, 0.8, 1.0\}$  of methane in the fuel blend, and pressures  $P = \{1, 5, 10, 15, 20, 25\}$  bar across the range of numerical flammability. For single fuel correlations, Eqs. 12 - 14 are used. In this set of equations, the formulation proposed by Hu et al. [23] for stoichiometric  $\beta$  pressure dependence is extended to the whole equivalence ratio range

$$S_u = S_{u0}(P/P_0)^{\beta}, \tag{12}$$

$$S_{u0} = W\phi^{\eta} e^{-\zeta(\phi - \sigma)^2},\tag{13}$$

$$\beta = (\beta_1 + \beta_2 \phi + \beta_3 \phi^2 + \beta_4 \phi^3) * (\beta_{p1} e^{-P/\beta_{p2}} - \beta_{p3}).$$
 (14)

This means that Eq. 12 is used to obtain distributions of  $S_{u0}$  and  $\beta$  from the laminar flame

speed  $S_u$  dataset for a given reference condition  $P_0$ , Eq. 13 is used to obtain the reference flame speed single fuel constants  $(W, \eta, \zeta \text{ and } \sigma)$  from the fitted  $S_{u0}$  distribution and Eq. 14 is used to obtain the coefficients  $\beta_1 - \beta_4$  and  $\beta_{p1} - \beta_{p3}$ . It is worth highlighting that particular choices of coefficients on Eq. 14 can decouple the pressure dependence  $(\beta_{p1} = 0 \text{ and } \beta_{p3} = -1)$  and/or reduce the order of  $\beta$ 's dependence with respect to the equivalence ratio  $(\beta_4 = 0)$ .

For dual fuel correlations, Eqs. 15 - 17 are used. The application of this set of equations is very similar to the one described for single fuel cases. The main differences are the use of a dual fuel laminar flame speed dataset for Eq. 15 and the introduction of reference flame speed regression parameters  $\nu$ ,  $\tau$ ,  $\epsilon$ , and  $\Omega$ . Also, in Eq. 16, methane's molar fraction  $X_{CH_4}$  is introduced as an independent variable. If deemed necessary, modifications may be introduced in Eq. 17 to account for a possible dependence of  $\beta$  with respect to fuel composition.

$$S_u = S_{u0}(P/P_0)^{\beta},\tag{15}$$

$$S_{u0} = (1 + \nu X_{CH_4}^{\tau}) W \phi^{\eta (1 - X_{CH_4})^{\epsilon}} e^{-\zeta (\phi - \sigma - \Omega X_{CH_4})^2}, \tag{16}$$

$$\beta = (\beta_1 + \beta_2 \phi + \beta_3 \phi^2 + \beta_4 \phi^3) * (\beta_{p_1} e^{-P/\beta_{p_2}} - \beta_{p_3}).$$
(17)

It is common in the literature associated with empirical correlations that parameters intrinsic to the fuel in the studied conditions are sought. In contrast, single fuel regression parameters W,  $\eta$ ,  $\zeta$  and  $\sigma$  are not used as the basis for dual fuel regressions in this work. These parameters are left unconstrained in order to obtain the best global fit.

While the matter of regression algorithms and initial conditions is not the focus of this work, it is worth noting that a standard MATLAB R2021b non-linear least squares method was used and

that the results may be sensitive to the initial guesses for the regression parameters.

#### 4. Results

205

The present section is divided in two parts. In the first one, the comparison between detailed chemistry calculations and experimental data is performed. Additionally, three-dimensional laminar flame speed maps are developed as functions of fuel blend composition and equivalence ratio for the best performing mechanism. In the second part, empirical correlations are evaluated for both single and dual fuel cases. Herein, existing correlation forms available in the literature and those proposed in this work are compared with detailed chemistry data and their performances are analyzed.

#### 4.1. Detailed chemistry analysis

For the comparisons between simulation results achieved with different reaction mechanisms and experimental data, the work of Davis and Law [32] is used, where experimental data of laminar flame velocity for a wide range of hydrocarbons under ambient conditions of temperature and pressure can be found. The uncertainty of the experimental data, as estimated by Davis and Law [32], is also considered.

For each mechanism, the comparison between the numerical results of the different transport models and the experimental data is shown in Fig. 1. In relation to the diffusion transport models, with the exception of unitary Lewis number, it can be observed that the main trend of the results is intrinsic to the mechanism. In other words, most of the diffusion model choices show modest influence on laminar flame speed results. Thus, the importance of using an adequate mechanism

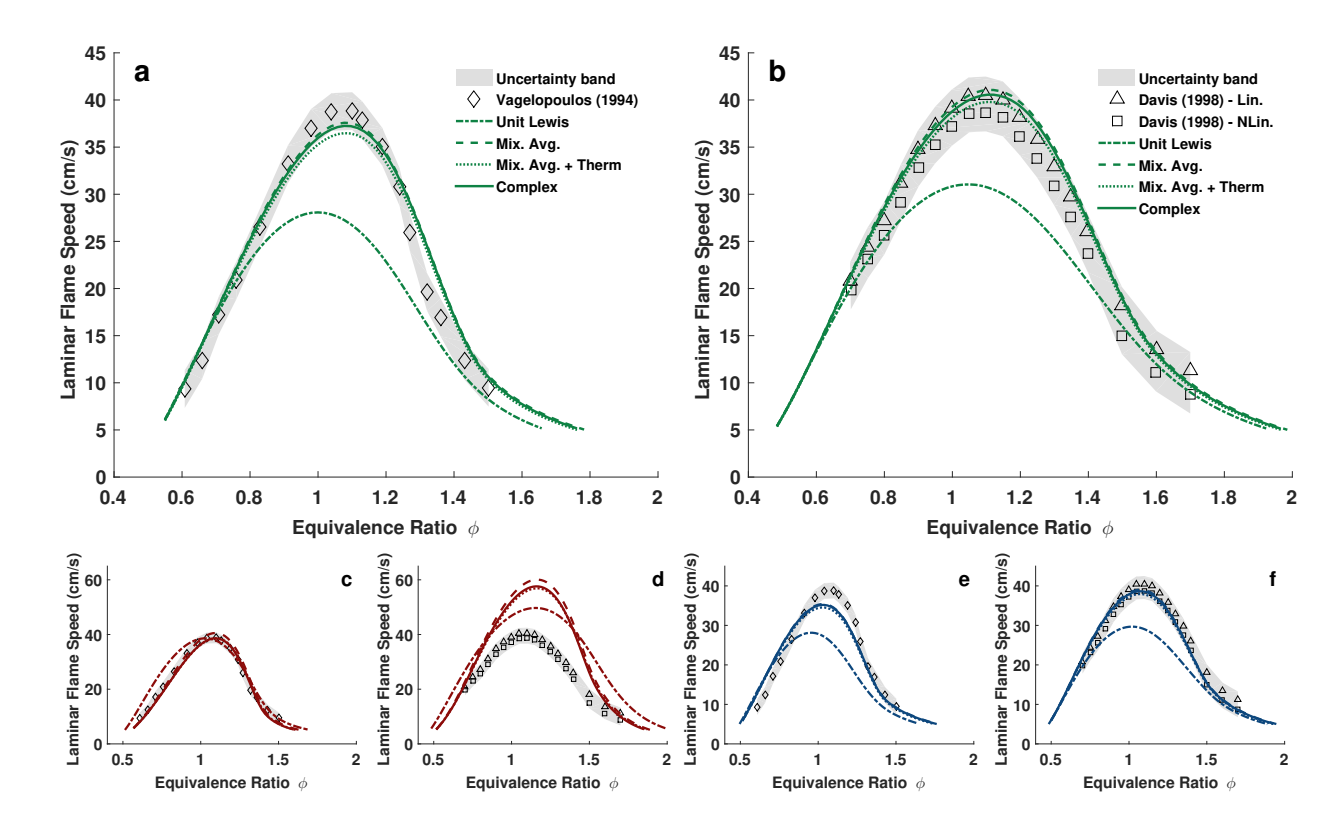


Figure 1: Laminar flame speed results computed with different mechanisms and diffusion transport models for methane and n-heptane. In green (a and b): Polimi TPRF; in red (c and d): Liu et al. [28]; in blue (e and f): Chaos et al. [29]. Markers: experimental data extracted from [32]; lines: simulation results at 1 atm and  $T_0 = 298K$ . The gray patches represent the uncertainty band as estimated in [32]. For n-heptane, the upper uncertainty boundary was estimated from Linear regression data, while the lower boundary was based on Non-Linear data.

for the desired application is restated. Still, it is possible to highlight the mixture averaged ordinary diffusion and complex transport models. Although Kee et al. [36] claim that there is no reliable method to model thermal diffusion using the mixture averaging approach, the results obtained are inconclusive in relation to this claim.

Differently from what is observed for unitary Lewis assumption, mixture averaged ordinary diffusion (Mix. Avg.) shows good results while keeping the computational cost reduced. The

complex transport formulation is more costly from a computational point of view, but offers satisfactory results with the greatest theoretical consistency among the available models. Due to the consistency of the model, the complex transport approach is applied hereafter.

From Fig. 1 it is possible to observe that the Liu et al. [28] mechanism presented clear deviations for the calculation of the laminar flame velocity of n-heptane, as it results in a clear overestimation of the experimental data. In contrast, the mechanisms of Chaos et al. [29] and of the Polytechnic University of Milan (Polimi) [30] achieved results close to the laminar flame velocity for n-heptane. With respect to laminar flame speed values of methane, it should be noted that, while the Liu et al. [28] mechanism shows results within the uncertainty limits, the results achieved with Chaos et al. [29] mechanism show some deviations from the available experimental data. The Polimi mechanism [30] provided results closer to the experimental data around stoichiometric conditions, but with a small overestimation in the rich region. Given the overall accuracy demonstrated by the Polimi mechanism, it is selected for further validation.

As done by Ranzi et al. [37], experimental data of pure methane, extracted from [15, 23, 38, 39] (300K), and n-heptane, extracted from [34] (353K) and [33] (373K), at elevated pressures are employed. Also, experimental data of methane/n-heptane blends at 1 bar and  $T_0 = 358K$  [35] are used for comparison with numerical results.

Validation of laminar flame speed predictions at high-pressure conditions is presented for methane and n-heptane in Fig. 2. For methane (Fig. 2a), very good agreement between experimental data and numerical results is found. For n-heptane, good agreement was found between the experimental data of Kelley et al. [34] and simulation results (Fig. 2b). Specifically at atmospheric pressure, only a small overestimation of laminar flame speeds around stoichiometric

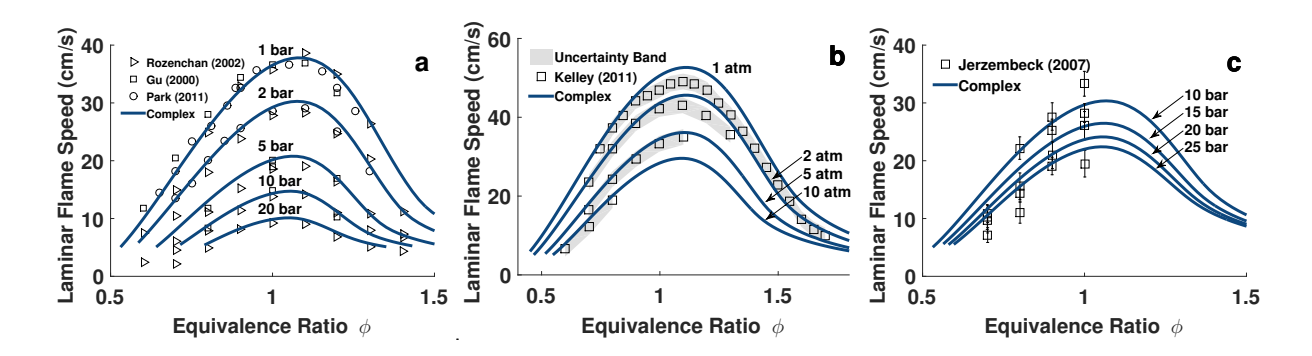


Figure 2: Polimi complex transport laminar flame speed validation for methane (a) and n-heptane (b and c) at elevated pressures. Markers: experimental data; lines: detailed chemistry; gray patch: uncertainty band as estimated in [34].

conditions can be observed. Regarding the comparison between detailed chemistry calculations and the experimental data of Jerzembeck et al. [33] (Fig. 2c), significant deviations can be seen. Even so, most of n-heptane laminar flame speed predictions are reasonably close to the corresponding experimental data error bars. Furthermore the comparison with the data of Kelley et al. [34] demonstrates the suitability of the numerical setup to predict laminar flame speeds of n-heptane at elevated pressures. It is worth highlighting that the results of Fig. 2 are very similar to those presented by Ranzi et al. [37], which employs a similar reaction mechanism developed at the Polytechnic University of Milan.

Regarding the laminar flame speed of methane/n-heptane blends, the Polimi mechanism is able to achieve good adherence with the experimental data presented in Fig. 3. However, at near-stoichiometric conditions, slight deviations are noticed. While this behavior may be associated to the mechanism, it is also relevant to point out an important aspect of this experimental dataset. As shown by Li et al. [35], their flame speed values are systematically lower around stoichiometric conditions when compared to the data of Dirrenberger et al. [40] for pure n-heptane. The dataset of Dirrenberger et al. [40] is the only laminar flame speed dataset for n-heptane presented by Li

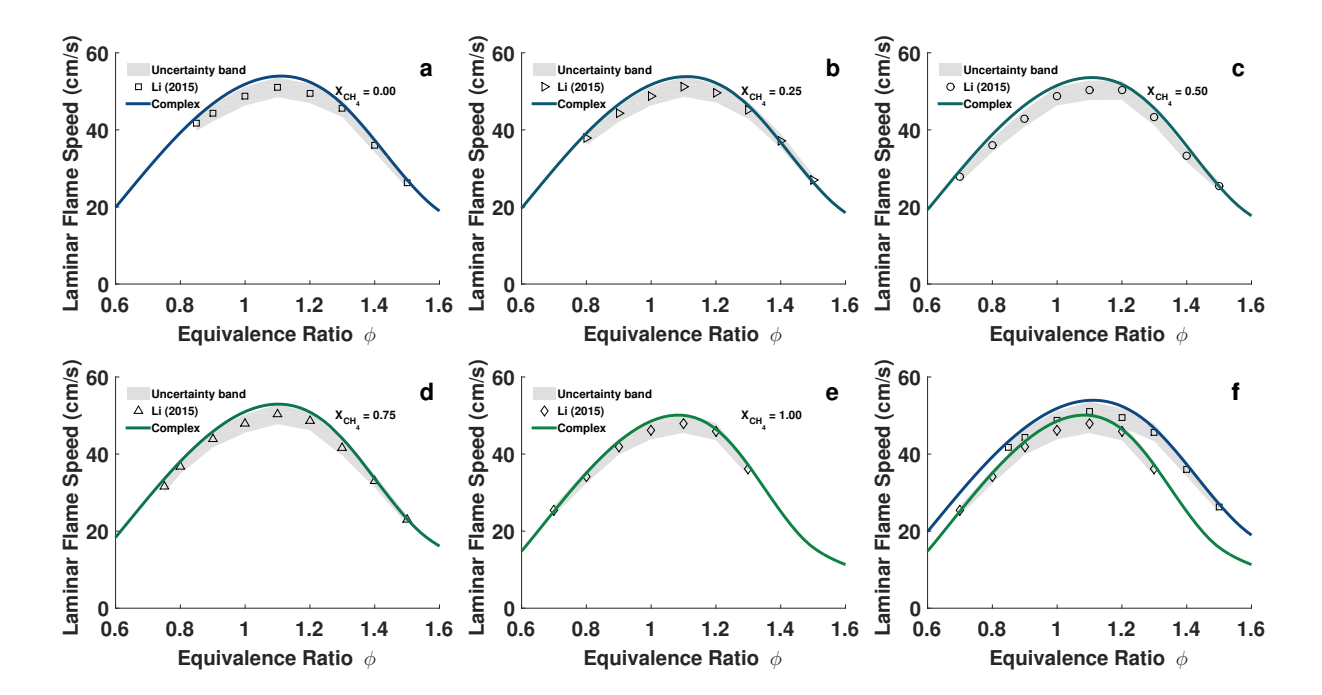


Figure 3: Polimi complex transport laminar flame speed validation for different methane/n-heptane blends (a - e). In f, experimental data and simulation results of both pure methane and n-heptane are compared. Markers: experimental data of Li et al. [35] (358K, 1 bar). Relative uncertainty of 5%, as stated in [35], was adopted.

et al. [35] which employs the same pressure and temperature specification as their experimental study. The reason of this systematic underestimation of flame speeds, when compared to the data of Dirrenberger et al. [40], is not clear. Even so, it is worth highlighting that the comparisons between simulation results and experimental data of Fig. 3 follow the same trend.

Figure 4 presents the laminar flame speed computed for dual fuel blends in terms of a three-dimensional map. Altogether, over two thousand one-dimensional flames were computed to construct these maps. From the achieved results, it is possible to draw some preliminary conclusions regarding dual fuel laminar flame speeds. The flame speed maps of Fig. 4 are smooth, free of noticeable oscillations in the blending region and bounded by single fuel laminar flame speeds. This indicates that the variations in the blending region scale with the difference between the lam-

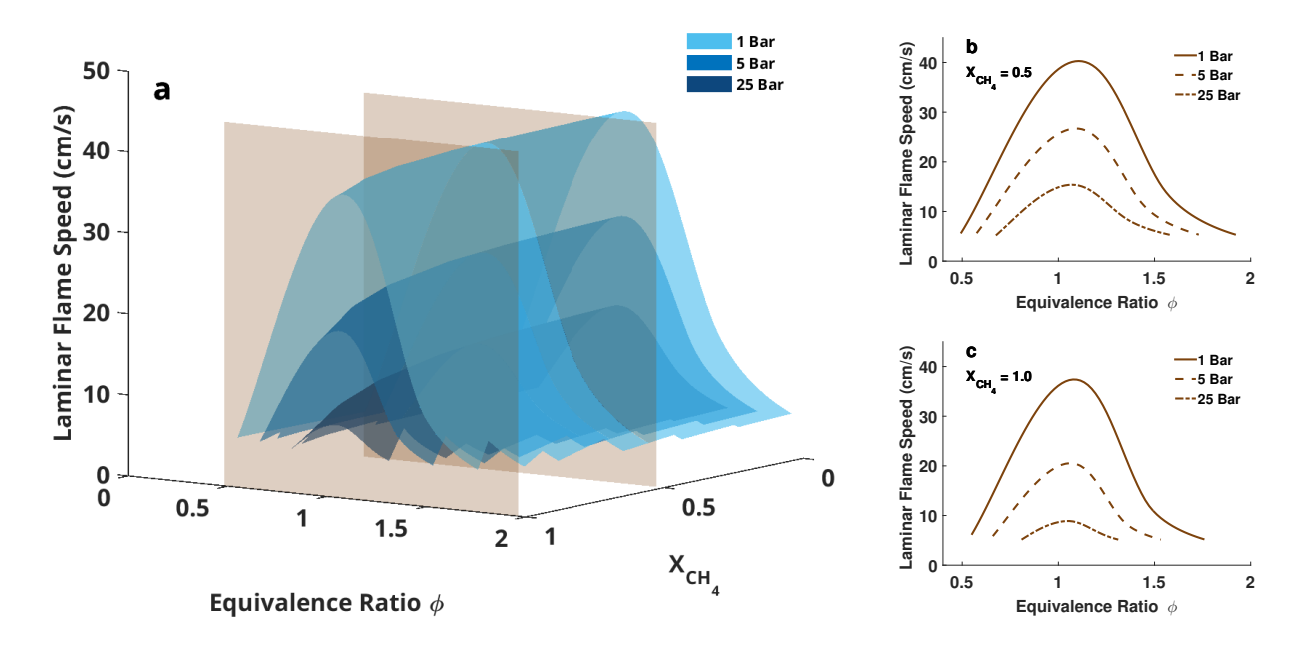


Figure 4: Polimi complex transport laminar flame speed maps for three different pressures (a). On the right, laminar flame speed slices corresponding to the brown rectangular patches (b and c).

inar flame velocities of each single fuel. This statement is corroborated by the forms of empirical equations found in the literature [6, 20], which suggest a monotonic behavior of flame velocity as a function of fuel composition.

It is important to highlight that the variation of the laminar flame speed profile  $(S_u \times \phi)$  along the molar fraction of methane  $(X_{CH_4})$  is not regular. This can be clearly noticed for high concentrations of methane  $(0.8 < X_{CH_4} < 1.0)$  on the surface of 5 bar. Such a non regular variation is also identified by comparing both line graphs presented on the right side of Fig. 4 and is more pronounced as the pressure increases. For brevity, only two curve graphs are presented, since the proportionality observed among the three pressure levels for  $X_{CH_4} = 0.5$  is preserved for lower values of  $X_{CH_4}$ . The change in proportion among the three pressure levels found for higher val-

ues of  $X_{CH_4}$  may be justified by the higher sensitivity of the laminar flame speed to pressure for methane. While the results do not indicate any unpredictable behavior for the laminar flame speed of methane-heptane blends, this is not guaranteed to be a general feature of dual fuel combustion. As previously mentioned, the obtained dataset can be directly used as an input for CFD simulations.

## 4.2. Empirical equation fit

Following the development of a laminar flame speed dataset for both single and dual fuel combustion in varied pressure conditions, empirical equations are fitted to the detailed chemistry dataset for a reference pressure  $P_0 = 1.0$  bar. Firstly, single fuel equations are fitted for an equivalence ratio range between 0.70 and 1.25 for methane and between 0.60 and 1.40 for n-heptane. Namely, Eq. 12 is used to obtain  $S_{u0}(\phi)$  and  $\beta(\phi, P)$  and Eqs. 13 and 14 are employed to fit  $S_{u0}(\phi)$  and  $\beta(\phi, P)$ .

The obtained fits are presented and the resulting laminar flame speeds are visually compared for both pressure independent  $\beta$  in Figs. 5a and 5d and pressure dependent  $\beta$  in Figs. 5b and 5e. Since the difference between quadratic and cubic forms of  $\beta$ 's dependence on equivalence ratio was small, only results for cubic regressions are presented. It is worth highlighting that methane and n-heptane are shown to have significantly different  $\beta$  values, which is justified by the change of proportion between laminar flame speed profiles observed in Fig. 4. Figures 5a and 5d indicate a strong pressure dependence of  $\beta$ , so that accounting for such a dependence significantly

<sup>&</sup>lt;sup>1</sup>This choice is made since the similarity between both quadratic and cubic forms may be case-specific. Therefore, we do not encourage the reader to assume that the cubic formulation is unnecessary without sufficient evidence.

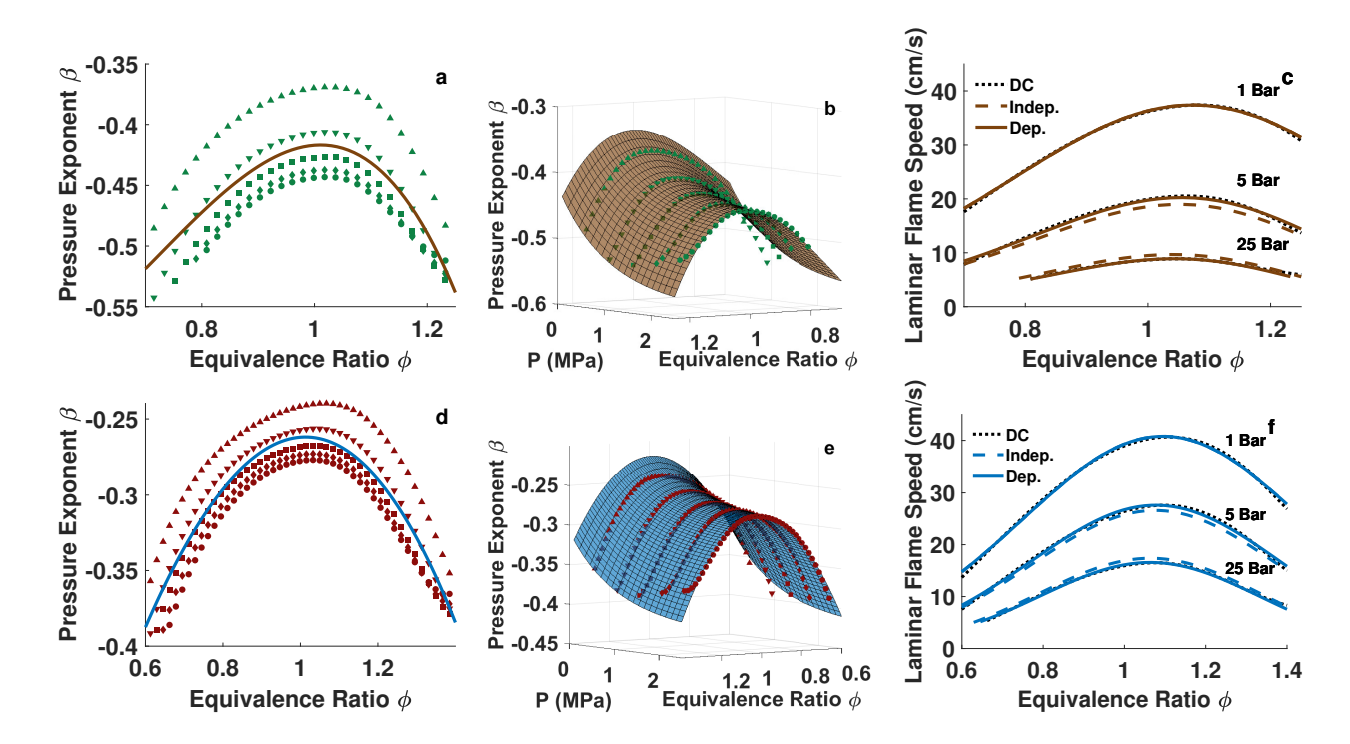


Figure 5: Pressure independent (a and d) and pressure dependent (b and e)  $\beta$  fits: Markers are obtained from Eq. 12. Lines and surfaces are fitted with Eq. 14. Each marker type refers to a specific pressure value. On the right, laminar flame speed comparison between detailed chemistry calculations and empirical regressions (c and f). Top (a, b and c): methane; bottom (d, e and f): n-heptane.

improves the fit in Figs. 5b and 5e. Even so, it is important to highlight that the extended pressure dependent  $\beta$  form corresponds to an exponential function of pressure, which does not account for cross influences of pressure and equivalence ratio.

Given the good performance of pressure dependent  $\beta$  fits, the improvement in empirical laminar flame speed calculations seen in Figs. 5c and 5f is expected. A direct consequence of assuming a mean value for  $\beta$  is that it is underestimated at low pressures and overestimated at high pressures, causing a mismatch between the calculated flame speeds and the flame speed dataset. As a result, by accounting for the pressure exponent's dependence on pressure, this mismatch vanishes.

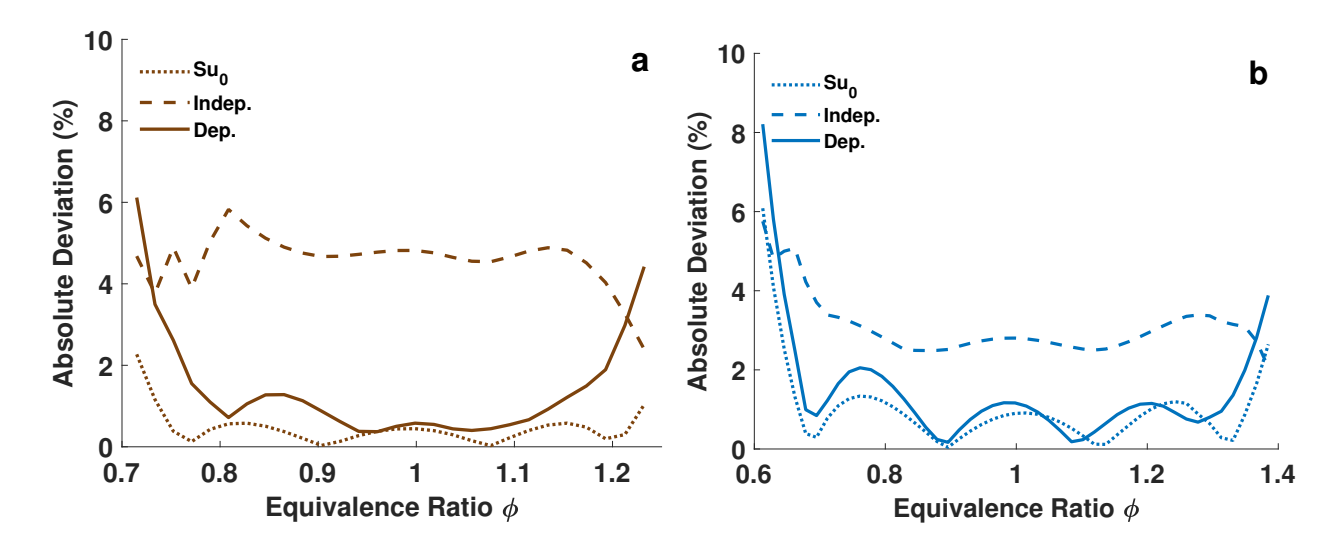


Figure 6: Pressure-averaged absolute deviation of laminar flame speed for methane (a) and n-heptane (b). Dotted line: reference flame speed; dashed line: pressure independent  $\beta$ ; solid line: pressure dependent  $\beta$ .

In Figs. 5c and 5f, reference pressure curves correspond to  $S_{u0}$  and can be used to analyze the estimation of this variable throughout the equivalence ratio (Eq. 13), as in this condition there is no influence of the pressure exponent (see Eq. 12). It can be seen that, for both methane and n-heptane, the form proposed by Ömer L. Gülder [7] well suits the data.

300

Figure 6 presents the pressure-averaged absolute deviation of laminar flame speed [ $\epsilon = 100 * (Su_{cor} - Su_{mec})/Su_{mec}$ ] in respect to the detailed chemistry dataset. Local oscillations can be seen in very lean conditions due to the pressure-averaging of the relative deviations. In Fig. 6, it is shown that laminar flame speed estimations are significantly improved through the use of pressure dependent correlations. Also, the good performance of Eq. 13 in the adopted equivalence ratio ranges is reinforced. However, deviations substantially increase in very lean and in rich conditions. This is due to changes in the shape of both reference laminar flame speed and pressure exponent distributions, which are not accurately captured by the used empirical forms. It is important to

highlight that the imposed equivalence ratio ranges were chosen in order to achieve comprehensive fits with modest deviations due to this change in shape. Even so, these deviations remain evident and demand further research. The coefficients for the regressions of  $S_{u0}$  and  $\beta$  for methane and n-heptane are presented in Tab. 2.

Table 2: Polimi single fuel laminar flame speed fit parameters

Fuel	W	η	ζ	σ	$oldsymbol{eta}_1$	$eta_2$	$oldsymbol{eta_3}$	$eta_4$	$eta_{p1}$	$eta_{p2}$	$eta_{p3}$
$CH_4$	53.1708	-2.3587	6.5100	1.2420	-0.1192	-2.5872	4.2330	-1.9411	-0.3011	0.9953	-1.0946
$C_7H_{16}$	40.5235	0.0788	4.0981	1.0862	-0.9627	1.2730	-0.4728	-0.1014	-0.2711	0.9999	-1.0712

For dual fuel regressions, a range between 0.65 and 1.30 is considered for the equivalence ratio. Equation 15 is used to obtain  $S_{u0}(\phi, X_{CH_4})$  and  $\beta(\phi, P)$ , while Eqs. 16 and 17 are employed to fit  $S_{u0}(\phi, X_{CH_4})$  and  $\beta(\phi, P)$ . The resulting fits are presented in Fig. 7 for pressure and composition independent (Fig. 7a) and pressure dependent  $\beta$  (Fig. 7b). Once again, only the cubic  $\phi$  dependence forms are shown, as the quadratic forms yielded similar results for the adopted  $\phi$  range.

In contrast to single fuel cases, Fig. 7b shows that there is a large scatter for pressure dependent  $\beta$ . This is caused by the influence of fuel composition on  $\beta$ 's distribution. As seen in Fig. 7b,  $\beta$  values are concentrated away from values respective to methane. Again, as for single fuel cases, this is justified by the change of proportion between laminar flame speed profiles observed in Fig. 4. Therefore, on a first attempt to account for the influence of the fuel composition, the pressure exponent is now treated as  $\beta(\phi, X_{CH_4})$  and a modified empirical form is proposed in Eq. 18. This

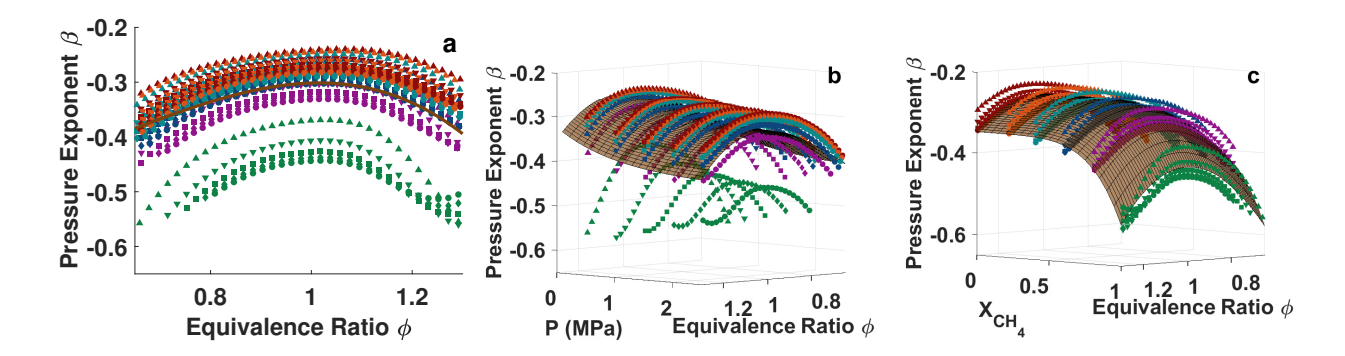


Figure 7: Pressure and composition independent (a), pressure dependent (b) and composition dependent (c)  $\beta$  fits: different markers are  $\beta$  points obtained from Eq. 15 in different pressure conditions and distinct marker colors correspond to distinct fuel compositions. Lines and surfaces are fitted with Eqs. 17 (a and b) and 18 (c).

expression is inspired by the binary blend form of reference flame speed fit (Eq. 16) and its results are shown in Fig. 7c.

$$\beta = (1 + \nu_{\beta} X_{2nd}^{\tau_{\beta}}) * (\beta_1 + \beta_2 \phi + \beta_3 \phi^2 + \beta_4 \phi^3).$$
 (18)

As shown in Fig. 7c, the reduced scatter of  $\beta(\phi, X_{CH_4})$  in relation to  $\beta(\phi, P)$  suggests that  $\beta$  has a stronger dependence on composition than on pressure for methane-heptane blends. As a result, the use of Eq. 18 results in a much better  $\beta$  fit, especially for high concentrations of methane. Whether this behavior remains true for other fuel blends is not clear and needs to be further investigated.

330

It is important to highlight that the composition dependent  $\beta$  (Eq. 18) form corresponds to an exponential polynomial function of composition, which does not include cross influences of composition and equivalence ratio. Accounting for both pressure and composition dependence for  $\beta(\phi, P, X_{CH_4})$  seems to be a very promising approach, but the higher dimensionality and probable cross influences may pose additional challenges for subsequent works.

In Fig. 8, the estimations of laminar flame speed resulting from the obtained fits are compared

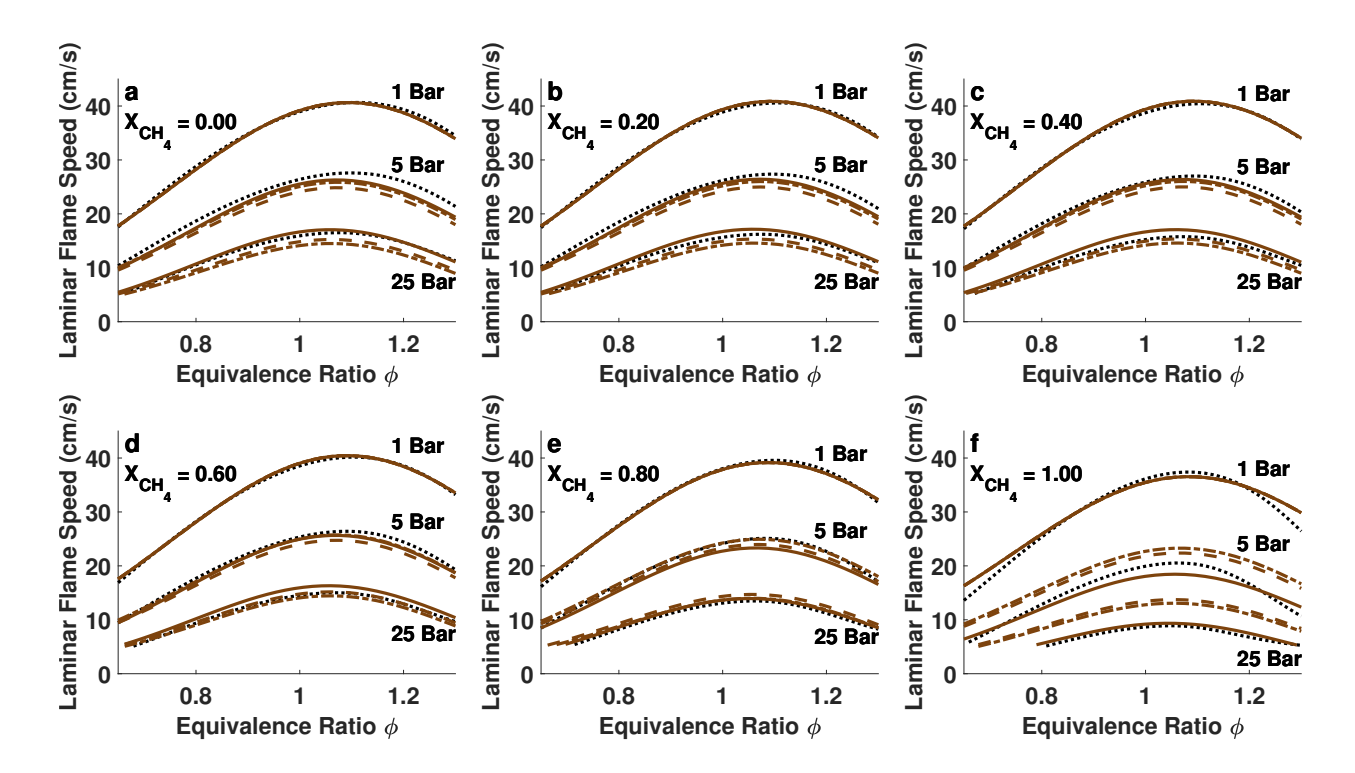


Figure 8: Comparison of laminar flame speed estimations between distinct pressure exponent formulations and detailed chemistry for different values of  $X_{CH_4}$ . Dotted line: detailed chemistry; dashed line: pressure and composition independent  $\beta$ ; dash-dot line: pressure dependent  $\beta$ ; solid line: composition dependent  $\beta$ .

with the detailed chemistry dataset. Once again, reference pressure (1 bar) curves can be used to analyze the estimation of  $S_{u0}$  throughout the equivalence ratio (Eq. 16), as in this condition there is no influence of the pressure exponent (see Eq. 15). It can be seen that, for all methane/n-heptane blends, the form proposed by Amirante et al. [6] well suits the data. Even so, it must be noted that significant deviations between the fitted  $S_{u0}$  and detailed chemistry calculations are found for pure methane (Fig. 8f) as the mixture departs from stoichiometry. For most cases (Figs. 8a - 8e), the estimations of all  $\beta$  formulations are visually similar. For pure methane, however, it is clear that the proposed formulation for composition dependent  $\beta$  performs better than the others, specially at higher pressures.

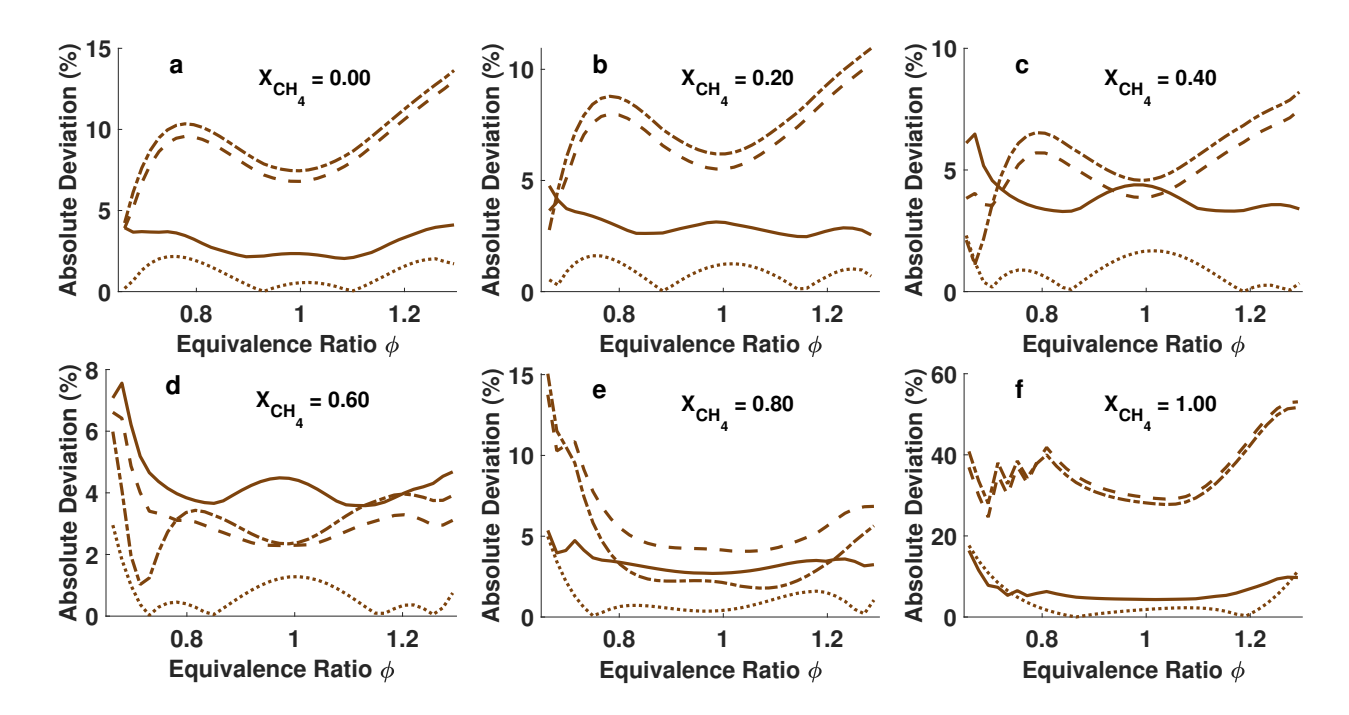


Figure 9: Pressure-averaged absolute deviation of the laminar flame speed for different values of  $X_{CH_4}$ . Dotted line: reference flame speed; dashed line: pressure and composition independent  $\beta$ ; dash-dot line: pressure dependent  $\beta$ ; solid line: composition dependent  $\beta$ .

In order to better analyze the performance of the different pressure exponent formulations, the estimations of laminar flame speed resulting from the obtained fits are compared through pressure-averaged absolute deviations in respect to the detailed chemistry dataset (Fig. 9). It is shown that the estimations are significantly improved through the use of composition dependent correlations, specially for high methane fractions. However, the pressure dependent form did not provide significant improvements, as the composition-wise scatter interferes with the pressure dependent fit. For intermediate blends (Figs. 9c - 9e), all  $\beta$  correlations performed similarly. This is caused by the fitting process of composition independent correlations. That is, these correlations are inherently averaged composition-wise as they are fitted. As a consequence, they tend to be more accurate for intermediate blends than for pure fuels. The composition dependent formulation, however, pro-

vides very similar results for these intermediate blends and is shown to be much more consistent throughout the whole fuel blend range.

The good performance of the reference flame speed fit (Eq. 16) in the adopted equivalence ratio range is clear. However, once again, deviations substantially increase in very lean and in rich conditions, specially for high methane fractions.

This is due to the very distinct reference flame speed profiles of methane and n-heptane, which are only partially captured by the used form. Additionally, changes in the shape of pressure exponent distributions in very lean and in rich conditions are not accurately captured by the used empirical forms and contribute to the observed deviations in Fig. 9.

As done for the single fuel investigations, it is important to highlight that the imposed equivalence ratio range was chosen in order to achieve a comprehensive fit with modest deviations. Even so, deviations remain evident and demand further research. The coefficients for the composition dependent regressions of methane and n-heptane dual fuel combustion, which are used in Eqs. 16 and 18, are splitted in Tabs. 3 and 4. It is important to highlight that the constructed dataset impacts on the proposed regressions and the carried out analyses. Thus, it is expected that, by using other datasets (from different mechanisms or even experimental data), different regression coefficients will be obtained when compared to those presented in this manuscript.

### 5. Summary and conclusions

In this work, empirical correlations for both single and dual fuel combustion are extended, proposed and analyzed. For single fuels, the pressure dependent form of Hu et al. [23] for the pressure exponent was extended to comprehend variations of the equivalence ratio. In dual fuel

Table 3: Dual fuel reference flame speed fit parameters

Fuel	ν	τ	W	$\eta$	$\epsilon$	ζ	$\sigma$	Ω
$CH_4 + C_7H_{16}$	-0.1151	3.6330	41.3048	-0.1643	1.8325	4.3048	1.1110	-0.0279

Table 4: Dual fuel  $\beta$  fit parameters

Fuel	$ u_eta$	$ au_eta$	$oldsymbol{eta}_1$	$eta_2$	$oldsymbol{eta_3}$	$eta_4$
$CH_4 + C_7H_{16}$	0.5782	4.9161	-0.9029	1.0119	-0.1245	-0.2502

context, a composition dependent formulation of the pressure exponent is proposed and clearly showed significantly improved results. To conduct the fitting process, a validated numerical setup was used to develop a laminar flame speed dataset of methane-heptane blends in various pressure conditions. The obtained dataset is also an outcome which can directly be used as an input for CFD simulations.

During the construction of the laminar flame speed dataset, three different reaction mechanisms were compared. Their predictions of laminar flame speed of methane and n-heptane were compared with available experimental data in ambient conditions [32]. As Polimi's mechanism was shown to be the most accurate overall, it was selected for additional validation in high-pressure

conditions and with different blend compositions. Due to its good performance, Polimi's mechanism was used for the development of the dataset. For this dataset, it was shown that the blending region is smooth and bounded by single fuel laminar flame speeds. Accordingly, as more pronounced the differences in behavior of laminar flame speed profiles of single fuels, as higher is the importance of accurately accounting for the effects of the intermediary fuel compositions in dual fuel context. Also, pressure exponent values were shown to be significantly different between methane and n-heptane.

In the single fuel context, the pressure dependent form of Hu et al. [23] was successfully extended for the whole equivalence ratio range. It was shown that by accounting for the pressure dependence of  $\beta$  (the pressure exponent) the estimations of the laminar flame speed are improved. Yet, in the dual fuel framework, it could be noticed that the exponent  $\beta$  is strongly dependent on the fuel composition. Consequently, the use of composition independent formulations resulted in very high deviations, specially for high methane fraction blends. A composition dependent formulation is proposed and shown to yield significantly improved results. In summary, results indicate that the proposed formulation, which is dependent on composition, should be preferred in dual fuel context instead of pressure dependent or even pressure and composition independent  $\beta$  formulations.

In both single and dual fuel contexts, deviations between empirical fits and detailed chemistry substantially increase for rich and very lean mixtures. In order to improve such fits, formulations must be modified to account for the change in behavior of laminar flame speed profiles in these conditions. To do so, existing correlations may need structural adjustments while new terms need to be included. Special attention is to be given to variables and to cross influences between them

which are still unaccounted for.

## 6. Acknowledgements

We are grateful to the Human Resources Program (PRH) of the Brazilian National Agency for Petroleum, Natural Gas and Biofuels (ANP) for supporting part of this research. This study was also financed in part by the Coordenação de Aperfeiçoamento de Pessoal de Nível Superior – Brasil (CAPES) – Finance Code 001.

#### References

420

- [1] E. E. de Pesquisa Energética], Balanço energético nacional (ben) 2020 balanço energético nacional (ben) 2020: Ano base 2019, 2020. URL: https://www.epe.gov.br/pt/publicacoes-dados-abertos/publicacoes/balanco-energetico-nacional-2020.
- [2] Y. Tan, K. V. Thambimuthu, M. A. Douglas, R. Mortazavi, Oxy-fuel combustion research at the canmet energy technology center, Proceedings of the 2003 5th International Symposium on Coal Combustion (2003) 550–554.
- [3] S. Singh, L. Liang, S. C. Kong, R. D. Reitz, Development of a flame propagation model for dual-fuel partially premixed compression ignition engines, International Journal of Engine Research 7 (2006) 65–75.
- [4] W. J. Pitz, N. P. Cernansky, F. L. Dryer, F. N. Egolfopoulos, J. T. Farrell, D. G. Friend, H. Pitsch, Development of an experimental database and chemical kinetic models for surrogate gasoline fuels, 2007. URL: https://www.sae.org/content/2007-01-0175/.doi:10.4271/2007-01-0175.
  - [5] F. Perini, Y. Ra, K. Hiraoka, K. Nomura, A. Yuuki, Y. Oda, C. Rutland, R. Reitz, An efficient level-set flame propagation model for hybrid unstructured grids using the g-equation, SAE International Journal of Engines 9 (2016) 1409–1424.
  - [6] R. Amirante, E. Distaso, P. Tamburrano, R. D. Reitz, Laminar flame speed correlations for methane, ethane, propane and their mixtures, and natural gas and gasoline for spark-ignition engine simulations, International Journal of Engine Research 18 (2017) 951–970.

- [7] Ömer L. Gülder, Correlations of laminar combustion data for alternatives s.i. engine fuels (1984) 23.
- [8] O. Colin, A. Benkenida, C. Angelberger, 3d modeling of mixing, ignition and combustion phenomena in highly stratified gasoline engines, Oil Gas Science and Technology 58 (2003) 47–62.
  - [9] O. Colin, A. Benkenida, The 3-zones extended coherent flame model (ecfm3z) for computing premixed/diffusion combustion, Oil Gas Science and Technology 59 (2004) 593–609.
- [10] L. Liang, R. D. Reitz, Spark ignition engine combustion modeling using a level set method with detailed chemistry, 2006. URL: https://www.sae.org/content/2006-01-0243/. doi:10.4271/2006-01-0243.
  - [11] F. Rahim, M. Elia, M. Ulinski, M. Metghalchi, Burning velocity measurements of methane-oxygen-argon mixtures and an application to extend methane-air burning velocity measurements, International Journal of Engine Research 3 (2002) 81–92.
- [12] A. S. Huzayyin, H. A. Moneib, M. S. Shehatta, A. M. Attia, Laminar burning velocity and explosion index of lpg-air and propane-air mixtures, Fuel 87 (2008) 39–57.
  - [13] L. Dressler, F. L. S. Filho, A. Sadiki, J. Janicka, Influence of thickening factor treatment on predictions of spray flame properties using the atf model and tabulated chemistry, Flow, Turbulence and Combustion 106 (2021) 419–451.
  - [14] M. Metghalchi, J. C. Keck, Burning velocities of mixtures of air with methanol, isooctane, and indolene at high pressure and temperature, Combustion and Flame 48 (1982) 191–210.

- [15] X. Gu, M. Haq, M. Lawes, R. Woolley, Laminar burning velocity and markstein lengths of methane–air mix-tures, Combustion and Flame 121 (2000) 41–58.
- [16] M. Elia, M. Ulinski, M. Metghalchi, Laminar burning velocity of methane–air–diluent mixtures, Journal of Engineering for Gas Turbines and Power 123 (2001) 190–196.
- [17] S. Liao, D. Jiang, Q. Cheng, Determination of laminar burning velocities for natural gas, Fuel 83 (2004) 1247–1250.
  - [18] P. Han, M. D. Checkel, B. A. Fleck, N. L. Nowicki, Burning velocity of methane/diluent mixture with reformer gas addition, Fuel 86 (2007) 585–596.
  - [19] P. Ouimette, P. Seers, Numerical comparison of premixed laminar flame velocity of methane and wood syngas,

Fuel 88 (2009) 528-533.

460

465

- [20] P. Dirrenberger, H. L. Gall, R. Bounaceur, O. Herbinet, P. A. Glaude, A. Konnov, F. Battin-Leclerc, Measurements of laminar flame velocity for components of natural gas, Energy and Fuels 25 (2011) 3875–3884.
- [21] L. Sileghem, V. Alekseev, J. Vancoillie, K. V. Geem, E. Nilsson, S. Verhelst, A. Konnov, Laminar burning velocity of gasoline and the gasoline surrogate components iso-octane, n-heptane and toluene, Fuel 112 (2013) 355–365.
- [22] M. Goswami, S. C. Derks, K. Coumans, W. J. Slikker, M. H. de Andrade Oliveira, R. J. Bastiaans, C. C. Luijten, L. P. H. de Goey, A. A. Konnov, The effect of elevated pressures on the laminar burning velocity of methane+air mixtures, Combustion and Flame 160 (2013) 1627–1635.
- [23] E. Hu, X. Li, X. Meng, Y. Chen, Y. Cheng, Y. Xie, Z. Huang, Laminar flame speeds and ignition delay times of methane-air mixtures at elevated temperatures and pressures, Fuel 158 (2015) 1–10.
  - [24] R. J. Varghese, H. Kolekar, V. R. Kishore, S. Kumar, Measurement of laminar burning velocities of methane-air mixtures simultaneously at elevated pressures and elevated temperatures, Fuel 257 (2019).
- [25] X. Han, Z. Wang, S. Wang, R. Whiddon, Y. He, Y. Lv, A. A. Konnov, Parametrization of the temperature dependence of laminar burning velocity for methane and ethane flames, Fuel 239 (2019) 1028–1037.
- [26] Y. Wang, A. Movaghar, Z. Wang, Z. Liu, W. Sun, F. N. Egolfopoulos, Z. Chen, Laminar flame speeds of methane/air mixtures at engine conditions: Performance of different kinetic models and power-law correlations, Combustion and Flame 218 (2020) 101–108.
  - [27] Y. Xie, Q. Li, A review on mixing laws of laminar flame speed and their applications on h2/ch4/co/air mixtures, International Journal of Hydrogen Energy 45 (2020) 20482–20490.
- [28] S. Liu, J. C. Hewson, J. H. Chen, H. Pitsch, Effects of strain rate on high-pressure nonpremixed n-heptane autoignition in counterflow, Combustion and Flame 137 (2004) 320–339.
  - [29] M. Chaos, A. Kazakov, Z. Zhao, F. L. Dryer, A high-temperature chemical kinetic model for primary reference fuels, International Journal of Chemical Kinetics 39 (2007) 399–414.
- [30] E. Ranzi, A. Frassoldati, A. Stagni, M. Pelucchi, A. Cuoci, T. Faravelli, Reduced kinetic schemes of complex reaction systems: Fossil and biomass-derived transportation fuels, International Journal of Chemical Kinetics

46 (2014) 512-542.

490

- [31] B. Somers, L. Somers, The simulation of flat flames with detailed and reduced chemical models, 1994. URL: http://alexandria.tue.nl/repository/books/420430.pdf.doi:10.6100/IR420430.
- [32] S. G. Davis, C. Law, Determination of and fuel structure effects on laminar flame speeds of c 1 to c 8 hydrocarbons, Combustion Science and Technology 140 (1998) 427–449.
  - [33] S. Jerzembeck, N. Peters, P. Pepiotdesjardins, H. Pitsch, Laminar burning velocities at high pressure for primary reference fuels and gasoline: Experimental and numerical investigation, Combustion and Flame 156 (2009) 292–301.
- [34] A. P. Kelley, A. J. Smallbone, D. L. Zhu, C. K. Law, Laminar flame speeds of c5 to c8 n-alkanes at elevated pressures: Experimental determination, fuel similarity, and stretch sensitivity, Proceedings of the Combustion Institute 33 (2011) 963–970.
  - [35] G. Li, J. Liang, Z. Zhang, L. Tian, Y. Cai, L. Tian, Experimental investigation on laminar burning velocities and markstein lengths of premixed methane-n-heptane-air mixtures, Energy Fuels 29 (2015) 4549–4556.
  - [36] R. Kee, M. Coltrin, P. Glaborg, H. Zhu, Chemically Reacting Flow: Theory, Modeling and Simulation, 2nd ed., John Wiley and Sons Inc., 2018.
  - [37] E. Ranzi, A. Frassoldati, R. Grana, A. Cuoci, T. Faravelli, A. P. Kelley, C. K. Law, Hierarchical and comparative kinetic modeling of laminar flame speeds of hydrocarbon and oxygenated fuels, 2012. doi:10.1016/j.pecs. 2012.03.004.
- [38] G. Rozenchan, D. L. Zhu, C. K. Law, S. D. Tse, Outward propagation, burning velocities, and chemical effects
  of methane flames up to 60 atm, 2002.
  - [39] O. Park, P. S. Veloo, N. Liu, F. N. Egolfopoulos, Combustion characteristics of alternative gaseous fuels, Proceedings of the Combustion Institute 33 (2011) 887–894.
  - [40] P. Dirrenberger, P. Glaude, R. Bounaceur, H. L. Gall, A. P. da Cruz, A. Konnov, F. Battin-Leclerc, Laminar burning velocity of gasolines with addition of ethanol, Fuel 115 (2014) 162–169.